

See discussions, stats, and author profiles for this publication at: <https://www.researchgate.net/publication/327692298>

Quantification of Aggregate Embedment in Chip Seals Using Image Processing

Article in *Journal of Transportation Engineering Part B Pavements* · December 2018

DOI: 10.1061/JPEODX.0000068

CITATIONS

10

READS

771

5 authors, including:



Ugurcan Ozdemir

Northeastern University

3 PUBLICATIONS 26 CITATIONS

[SEE PROFILE](#)



M. Emin Kutay

Michigan State University

122 PUBLICATIONS 1,893 CITATIONS

[SEE PROFILE](#)



Derek Hibner

Michigan State University

3 PUBLICATIONS 33 CITATIONS

[SEE PROFILE](#)



Michele Antonio Lanotte

Khalifa University

43 PUBLICATIONS 260 CITATIONS

[SEE PROFILE](#)

Some of the authors of this publication are also working on these related projects:



Tire-Pavement Interaction Noise [View project](#)



Development of a fast and cost-effective asphalt mixture fatigue test system [View project](#)

Quantification of Aggregate Embedment in Chip Seals Using Image Processing

Ugurcan Ozdemir, S.M.ASCE¹; M. Emin Kutay, M.ASCE²; Derek Hibner, A.M.ASCE³; Michele Lanotte, M.ASCE⁴; and Yogesh Shamsunder Kumbarger, S.M.ASCE⁵

Abstract: Chip seals are among the most popular preventive maintenance techniques implemented by many Departments of Transportation (DOTs), county road departments, and cities. The deteriorated pavement surface is sprayed with an asphalt emulsion or binder, and then a layer of uniformly graded aggregates is spread and compacted. Curing is required before opening the road to traffic to enhance bonding between aggregate particles and asphalt binder. Percent embedment of aggregate particles into the thin bituminous layer is one of the most significant parameters affecting the performance of asphalt chip seals. Bleeding or aggregate loss may be encountered in chip seal applications depending on the aggregate percent embedment. The main objective of this study is to develop a standard test procedure to directly calculate the aggregate percent embedment into the asphalt binder in a chip seal project via digital image analysis. Three image analysis algorithms were developed and used to analyze chip seal samples. Thirty-nine cores were collected from six different locations in Michigan and analyzed. The analyses were also performed using the sand patch tests and laser texture scanning techniques. DOI: [10.1061/JPEODX.0000068](https://doi.org/10.1061/JPEODX.0000068). © 2018 American Society of Civil Engineers.

Author keywords: Chip seal; Asphalt; Emulsion; Pavement preservation; Percent embedment.

Introduction

Since the 1920s, chip seal applications have been used as a method for resurfacing pavements. Early projects involved the use of chip seals in the construction of new low-volume roads, but in the last two decades, this methodology has turned into a maintenance and preservation treatment of existing deteriorated pavements. Researchers have also studied and verified the effectiveness of chip seal treatment with respect to lifecycle analysis (Zaniewski and Mamlouk 1996). Chip seal applications consist of distributing hot asphalt binder or emulsion over the surface of an existing pavement, and then uniformly graded aggregates (chips) are spread over the surface and compacted. The hot asphalt fills and seals existing cracks and establishes a waterproof layer to reduce moisture infiltration and aging of the underlying pavement structure, and aggregates provide the required skid resistance (Janisch and Gaillard 1998). Chip seal applications require simple technologies and low material quantity. For this reason, many Departments of Transportation (DOTs) and county and city road departments prefer this low-cost preventive maintenance method to improve the

serviceability level and life of deteriorated pavements (Gransberg and James 2005).

Despite the growing number of chip seal projects in the United States, a unified design method still does not exist. Hanson (1934), in the early 1930s, developed for the first time a procedure to design chip seal applications. Results of his study focused on two important concepts: voids between aggregates and voids filled with asphalt. Hanson suggested three target values for the percentage of air voids (AV) between aggregates: 50% after aggregate spreading, 30% after rolling, and 20% after curing. Additionally, asphalt binder should fill 60%–75% of the voids between aggregates. Hanson's research served as the basis for Kearby (1953)'s study, in which the notions of application rate and percent embedment were used for the first time in the design procedure of chip seal. The main result of that study was a nomograph, which uses percent embedment values and voids between aggregate as inputs for the calculation of binder and aggregate application rates. Research performed by McLeod et al. (1969) represents another milestone in the definition of a design procedure for chip seal applications. Empirical equations were defined to estimate binder and aggregate application rates. Although the aggregate percent embedment was not a direct input in these equations, it was considered in the calculation of the traffic correction factor needed for evaluation of the binder application rate.

Many researchers have studied the effect of type of aggregates on mean profile depth (MPD) (which is related to percent embedment) of chip seals (Adams and Kim 2014; Aktaş et al. 2013). These studies concluded that when lighter aggregates are used, the MPD tends to reduce quickly (i.e., percent embedment increases) with traffic loading, as opposed to more dense aggregates (such as from granite). Furthermore, the type of asphalt binder was also found to affect the chip retention and embedment (Abedini et al. 2017; Lee and Kim 2012). As part of those studies, the relationship between aggregate percent embedment values and main chip seal distresses was investigated. Results highlighted that chip seal applications having an aggregate percent embedment level below

¹Formerly, Graduate Student, Dept. of Civil and Environmental Engineering, Michigan State Univ., East Lansing, MI 48824.

²Associate Professor, Dept. of Civil and Environmental Engineering, Michigan State Univ., East Lansing, MI 48824 (corresponding author). ORCID: <https://orcid.org/0000-0002-0575-1917>. Email: kutay@msu.edu

³Formerly, Graduate Student, Dept. of Civil and Environmental Engineering, Michigan State Univ., East Lansing, MI 48824.

⁴Formerly, Postdoctoral Associate, Dept. of Civil and Environmental Engineering, Michigan State Univ., East Lansing, MI 48824.

⁵Graduate Student, Dept. of Civil and Environmental Engineering, Michigan State Univ., East Lansing, MI 48824.

Note. This manuscript was submitted on June 7, 2017; approved on April 24, 2018; published online on September 6, 2018. Discussion period open until February 6, 2019; separate discussions must be submitted for individual papers. This paper is part of the *Journal of Transportation Engineering, Part B: Pavements*, © ASCE, ISSN 2573-5438.

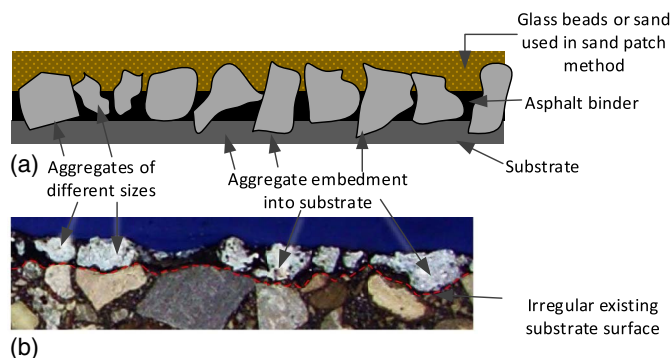


Fig. 1. Aggregate penetration into substrate: (a) conceptual representation of a chip seal cross section; and (b) cross section of a chip seal sample collected from the field.

50% showed insufficient bonding between asphalt binder and aggregate and were more susceptible to aggregate loss. On the other hand, chip seals with an aggregate percent embedment level above 70% exhibited bleeding.

The relationship among percent embedment, application rate, and distresses has recently guided the development of other chip seals design methodologies (Gaughan 2001; Roberts and Nicholls 2008; Shuler 2011). In these methods, percent embedment criteria (within the range of 40%–70%) have been established to have a certain impact on the calculation of aggregate and binder application rates. However, even if the importance of the percent embedment has been widely acknowledged, the practical difficulties encountered so far for its assessment have privileged the selection of application rates as main design factors. These rates, in fact, are often specified by state agencies, whereas the rest of the design factors are predominantly based on experience. As evidence of these difficulties, only two test methods are currently available for the estimation of aggregate percent embedment, both of which perform an indirect estimation of the percent embedment. These two tests are the sand patch test, recommended in the *Manual for Emulsion-based Chip Seals for Pavement Preservation* (Shuler 2011), and the surface texture laser scanning test. However, even though they are relatively straightforward, percent embedment calculated using these two methods ignores the irregularities on the existing surface, leakage of the emulsion into the existing pavement surface, size distribution of aggregates, aggregate penetration into the substrate, and aggregates that are not aligned along their flattest dimension (Fig. 1).

Several studies have utilized image processing methods to evaluate chip seals. Kim and Lee (2006) determined the optimum rolling patterns on asphalt chip seals using macrotexture properties obtained from image analysis techniques. Kodippily et al. (2010) identified the role of volumetric properties and distribution of air voids in chip seals using an image-based algorithm, and Wielinski et al. (2011) used this approach to determine the aggregate retention on the chip seal surface. Even though this approach has been used for asphalt chip seals, none of the available research studies have focused on the percent embedment calculation.

The objective of this study is to develop image-based algorithms to directly measure aggregate embedment in asphalt chip seals (Ozdemir 2016). Three image-based algorithms were developed to quantify aggregate embedment. Numerous field chip seal samples were analyzed using the newly developed algorithms. These samples were also evaluated using the sand patch test and laser texture scanning methods.

Image Processing and Analysis Methods

Sample Preparation and Image Acquisition

Fig. 2 illustrates the overall procedure for sample preparation and image acquisition. As shown, a chip seal core is first obtained from the field. In the laboratory, the chip seal application and underneath layer are separated in order to process this portion only. Using a lab saw, vertical cuts are made to obtain slices with clean faces. This produces a clear view of the different phases (aggregate and chip seal binder). Then, the digital images are captured using a digital camera. As mentioned previously, the procedure starts with a horizontal cut to reduce the height of the sample so that a small tile saw can be used to slice the sample vertically [Fig. 2(b)]. For cutting the 150-mm (6-in.) diameter cores horizontally, a traditional asphalt diamond saw was used [508-mm (20-in.) diameter wet slab saw with maximum cutting speed of 1,150 revolutions per minute (rpm)]. The sawing was done in wet condition using tap water. The final height of the shortened chip seal core was approximately 38.1 mm (1.5 in.). The second cutting operation was vertical slicing [Fig. 2(c)]. For cutting the samples vertically, a small tile saw was used [177.8-mm (7-in.) diameter wet tile saw with maximum cutting speed of 3,450 rpm]. This tile saw was purchased from a local hardware store. Typically, five slices can be obtained from a 150-mm-diameter core [Fig. 2(d)]. An image of each slice face can be acquired and analyzed, providing a total of eight images per core. Once the slices (cross sections) are obtained from the cores, a document camera is used to capture pictures [Fig. 2(e)].

To allow the algorithms to work in the proper manner, the laboratory technician must respect and follow certain sample preparation criteria: First, the top of the chip seal surface should be covered with a uniformly colored substance. For this purpose, a blue modeling compound, commonly named as play dough, has been used. Second, a good color contrast must be ensured between the emulsion residue binder and chip seal aggregates. Moreover, the quality of the captured pictures is highly affected by light reflection on both the binder and aggregates, which must be avoided. Thus, in order to finalize the image acquisition process, many imaging techniques have been tested before getting good imaging results. Different light conditions and professional cameras were evaluated. At the end, a document camera (e.g., Elmo Model TT02RX, Elmo USA, Plainview, New York) with an indoor white fluorescent light was selected. A desirable cross-section image is illustrated in Fig. 2(f).

Another issue that may be encountered in some field cores is the appearance of the surface of certain types of aggregates after slicing. For example, blast-furnace slag aggregates are quite dark and have numerous pores. This poses a challenge for the image-based algorithms. Fig. 3(a) shows a problematic cross section. After several trials for improving the aspect of the cross sections, painting aggregates using a fine-tip board marker (e.g., DecoColor, Uchida of America, Torrance, California, opaque paint marker with white color code 300—S White) was found to be promising. Fig. 3(b) illustrates the cross sections after painting. Painting the aggregates with fine tip board marker was relatively quick because the white ink flows out of the marker and spreads easily on the aggregate surface.

Finding the Pavement Substrate in the Image

The first critical step developed in the algorithms was to find the profile (macrotexture) of the surface of the existing road pavement underlying the chip seal application. For that purpose, a number of points were manually selected just below the emulsion layer on the existing pavement, and care was taken to select sharp changes of color, as shown in Fig. 4(a).



(a)



(b)



(c)



(d)

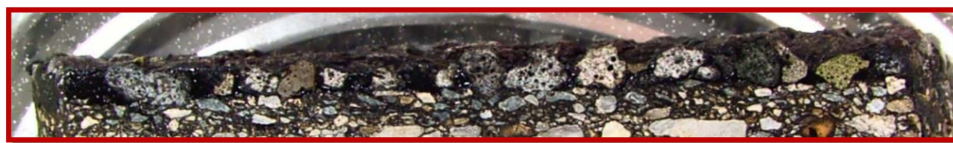


(e)

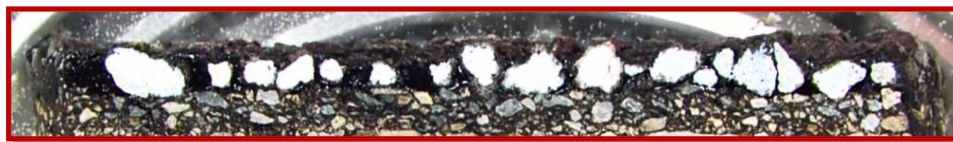


(f)

Fig. 2. Sample preparation and image acquisition: (a) field coring; (b) horizontal cutting; (c) vertical slicing; (d) core slices; (e) image acquisition of the core slice; and (f) desired image of the cross section.



(a)



(b)

Fig. 3. (a) Cross section of a chip seal made with blast-furnace slag; and (b) cross section after painting with fine-tip pen.

These points were used as input in the algorithm, which connects them to create a discrete curve [multiple straight lines shown in red in Fig. 4(b)]. Then, above the red curve, the algorithm creates a parallel line with an offset of 15 pixels [blue line in Fig. 4(b)]. At this point, the algorithm converts the color picture into a grayscale image and eliminates the eventual noise using some filtering techniques (e.g., Gaussian filter and image sharpening). Then, the algorithm starts to analyze the image from the blue line toward the substrate (top to down in the image). The result of this analysis is a plot of the color intensity profile for each x -coordinate of the pixels located on the blue line [Fig. 4(c)]. When the last pixel value less than 0.2 is found, it is taken as the transition point between the

existing pavement and chip seal surface emulsion. This process is repeated for all columns of pixels (from left to right) to obtain the existing pavement profile shown in Fig. 4(d). Theoretically, because the binder is black, it should have a pixel intensity of 0 out of 255, where 255 corresponds to pure white (any pixel intensity between 0 and 255 corresponds to different shades of gray). Therefore, the normalized pixel intensity of $0/255 = 0$ should correspond to asphalt binder. However, depending on brightness of the image, binder color intensity may be slightly greater than 0. After looking at many images, it was determined that the normalized pixel intensity of 0.2, which corresponds to $0.2 \times 255 = 51$, is about the maximum value for a binder. Any intensity larger than

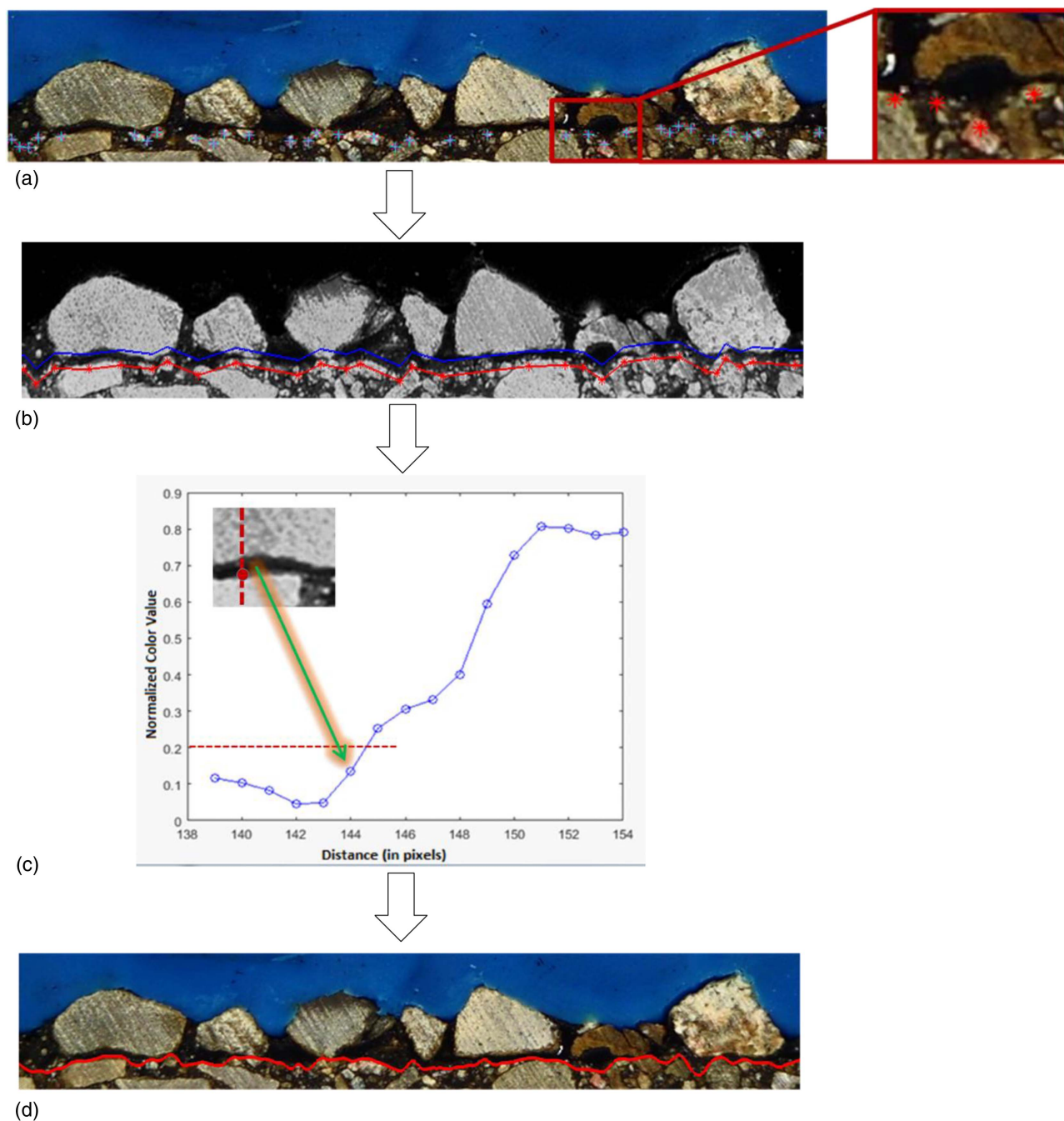


Fig. 4. Steps of determining the existing pavement surface.

51 usually corresponds to other objects (e.g., dark aggregates), and therefore was not classified as binder.

Once the pavement substrate is recognized, the layer of chip seal application can be analyzed.

Computing Percent Embedment: Peak and Valley Method

In this method, the chip seal surface profile (macrottexture) is determined by exploiting the color contrast between the blue play dough and the aggregates (Fig. 5). Then, on this line, both local maxima and minima values are found by the algorithm. Peak values are assumed to be the top of the aggregates and valley values are assumed to be the top of the binder layer. Because the algorithm

recognizes the local maxima and minima values, not all of them represent the top of the aggregate or the top of the binder layer. To limit the number of these points, a threshold value defined by the user (named here as delta) is used. The algorithm analyzes the difference of height between two adjacent peak and valley points; if this is smaller than the delta value defined by the user, points are ignored.

At this stage of the analysis, the algorithm has three sets of coordinates: the existing pavement (described in the previous section), the peak points, and the valley points. The average of the existing pavement y-coordinates is used to draw the existing substrate reference line [Fig. 5(b)], and the average of the peak points and valley points are used to draw the peak (aggregate) line and valley (binder) line [Fig. 5(c)], respectively. Then, the aggregate

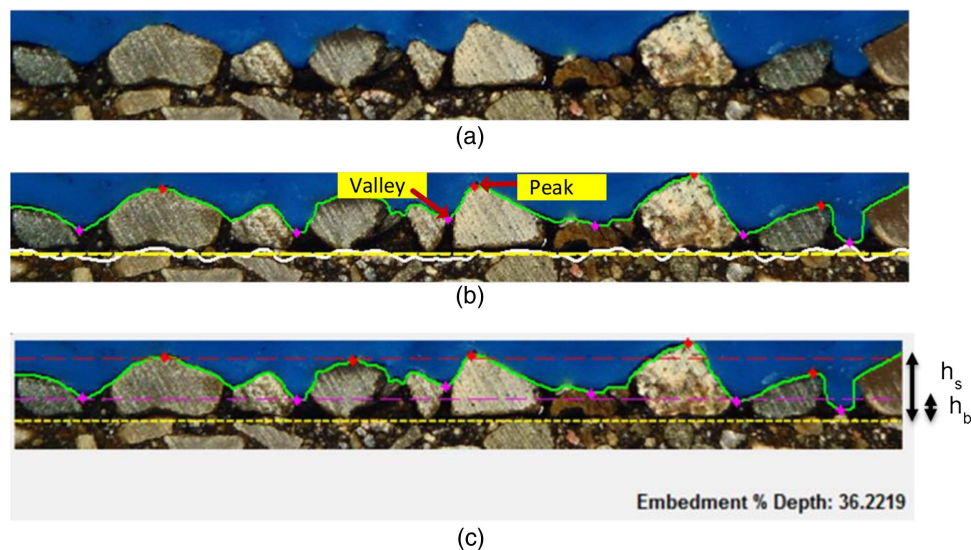


Fig. 5. Steps of the peak and valley method: (a) original image; (b) finding peak and valley points—existing pavement's determination; and (c) embedment depth calculation.

height (h_s) and binder height (h_b) are calculated by subtracting the existing pavement line from the peak height and binder height. The percent embedment is finally calculated as follows:

$$PE_{pv}(\%) = \frac{h_b}{h_s} \cdot 100 \quad (1)$$

where PE_{pv} = percent embedment based on peak/valley method; h_b = average binder height; and h_s = average aggregate height.

Computing Percent Embedment: Each-Aggregate Method

This algorithm computes the percent embedment of each individual aggregate and performs a statistical analysis to compute the percent embedment distribution. The algorithm works as follows:

- The chip seal aggregates are isolated for the analysis by converting to black color all the pixels that belong to the existing surface [Fig. 6(a)].
- The true color [Red Green Blue (RGB)] image is sharpened to have the different features of the image (e.g., edges) clearly visible and sharper. Then, the image is converted to grayscale, and all the components of the samples including the blue play dough turn dark except for the aggregates, which remain lighter in color [Fig. 6(b)].
- A two-dimensional (2D) median filtering technique is used to modify the grayscale image and remove irregularities [Fig. 6(c)]. The resulting image is then converted into a black and white image. As shown in Fig. 6(d), some holes may appear on the aggregate surface that may affect the correct processing of the sample. A series of dilation and contraction operations are performed to overcome this problem, and the resulting image is shown in Fig. 6(e).
- Finally, the aggregates are separated using the watershed transformation [Fig. 6(f)].

Aggregate properties such as x - and y -coordinates of their perimeters can easily be computed once they appear to be islands of white pixels in an image. This was accomplished using the regionprops command in MATLAB 2015a. Once the perimeter pixels of individual aggregates are obtained, the intersection between

the chip seal surface line and any aggregate perimeter is determined as shown in Fig. 7(a). The left and right end points of intersecting lines for each aggregate are assumed to be the peak binder heights. The binder height for each aggregate is the average of two binder peak points from the base (lowest y -coordinate) of the corresponding aggregate [Fig. 7(b)].

The height of each aggregate is calculated by subtracting the lowest y -coordinate from the highest y -coordinate for the corresponding aggregate [Fig. 7(b)]. The percent embedment for each aggregate is calculated by dividing the binder height by the aggregate height

$$P_{e(i)}(\%) = \frac{h_{b(i)}}{h_{s(i)}} \cdot 100 \quad (2)$$

where $P_{e(i)}$ = percent embedment of i th aggregate; $h_{b(i)}$ = binder height for the corresponding to the i th aggregate; and $h_{s(i)}$ = i th aggregate height. After calculating the $P_{e(i)}$ values for each aggregate, the average percent embedment is computed as follows:

$$PE_{EA}(\%) = \frac{\sum_i P_{e(i)}}{N} \quad (3)$$

where PE_{EA} = percent embedment based on each aggregate; $P_{e(i)}$ = percent embedment of i th aggregate; and N = number of aggregates in a cross section.

Computing Aggregate Surface Coverage by the Binder

A third algorithm has been developed in this study, called Aggregate-Surface Coverage. Because the adhesion between the aggregates and asphalt binder prevents chips from being pulled out, it is hypothesized that the probability of aggregate loss decreases as the portion of aggregate surface covered by asphalt increases. The algorithm developed in this study first computes each aggregate's coordinates as well as the perimeter pixels. For each aggregate, the center coordinates (x - and y -coordinates) are calculated, whereas for each perimeter coordinate, the direction from center to the perimeter is obtained (Fig. 8). Then, the algorithm records the color intensity at five pixels outside each perimeter coordinate. If the pixel intensity does not correspond to the blue color,

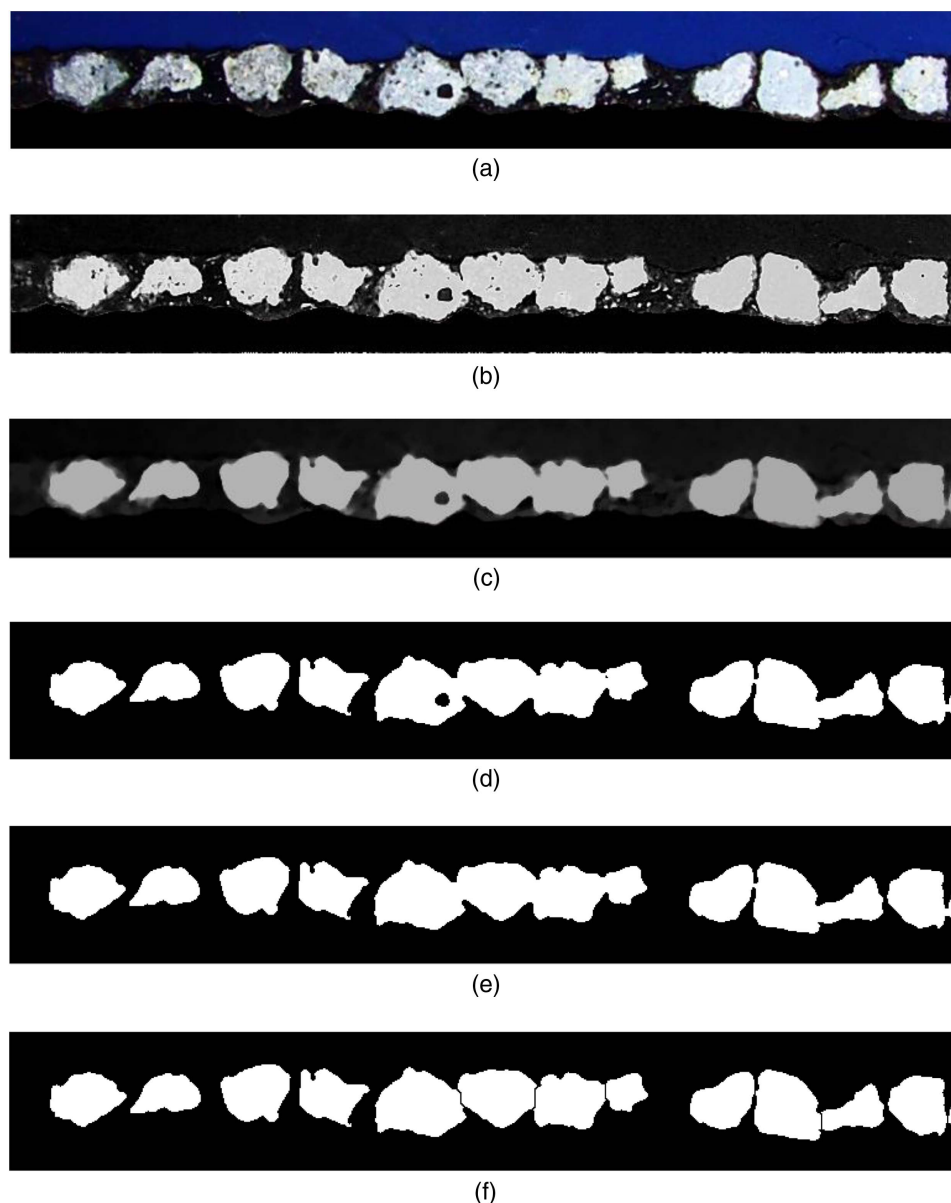


Fig. 6. Steps of identifying individual aggregates: (a) Step 1: existing pavement section removed; (b) Step 2: image sharpened and converted to grayscale; (c) Step 3: application of the 2D median filtering; (d) Step 4: grayscale image converted into a black and white image; (e) Step 5: holes in aggregate surface filled; and (f) Step 6: separation of aggregates through watershed transform.

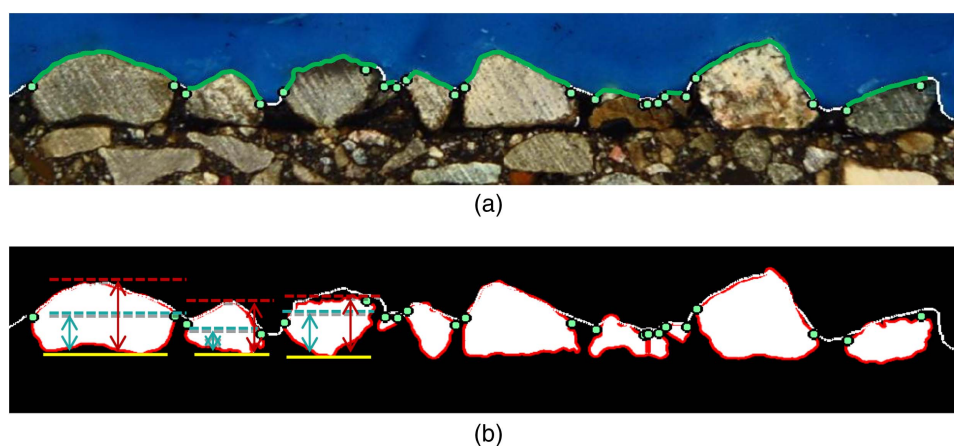


Fig. 7. Computation of percent embedment of each aggregate: (a) intersection line; and (b) calculation of the percent embedment.

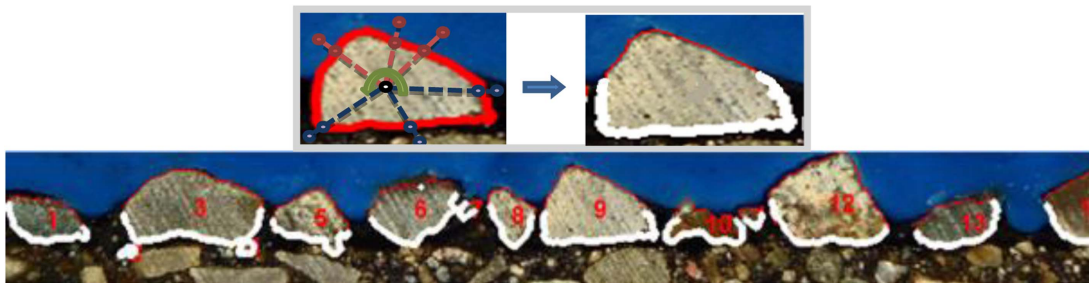


Fig. 8. Algorithm computing the portion of the aggregate surface covered by the binder.

it assumes that the perimeter coordinate is in contact with the binder (i.e., covered by the binder). The average of these coverage areas gives the overall aggregate surface coverage area

$$PC_{EA}(\%) = \frac{\left(\sum_i \frac{(A_{BS})_i}{(A_{PS})_i} \cdot 100 \right)}{N} \quad (4)$$

where PC_{EA} = average percent coverage of the binder (based on analysis of each aggregate); $(A_{BS})_i$ = binder coverage around the i th aggregate; $(A_{PS})_i$ = perimeter the i th aggregate; and N = total number of aggregates in a cross-sectional image. The percent coverage of the binder around each aggregate is shown in Fig. 8.

Development of a Standalone Software Package

All the algorithms described previously were implemented into a standalone software named CIPS developed under the MATLAB programming language. The main input is the digital image of the vertical cross section of the chip seal sample, and the main output of the analysis are the percent embedment and percent binder coverage,

which were described previously. It was designed to be a very simple, with no more than seven steps to determine all the parameters. After opening the software, the user has to begin from the left-most menu bar option (named File) and load the input image of chip seal sample. Subsequently, the user is prompted for calibration and image cropping, followed by the image processing algorithms that have been explained in preceding sections. Under the Results option, the percent embedment using all the three methods can be viewed by the user. Moreover, additional outputs such as binder and aggregate application rates have also been included in the software. A screenshot of CIPS is shown in Fig. 9. The analysis results can be exported to Microsoft Excel files. Finally, the software can compute the percent within limits (PWL) for each of the parameters using the Microsoft Excel outputs of numerous vertical slices.

Validation of the Image Processing Algorithms

In an effort to validate the aforementioned algorithms, first, a synthetic chip seal image was generated such that the percent embedment was exactly 50%. This image was input to the algorithms, and

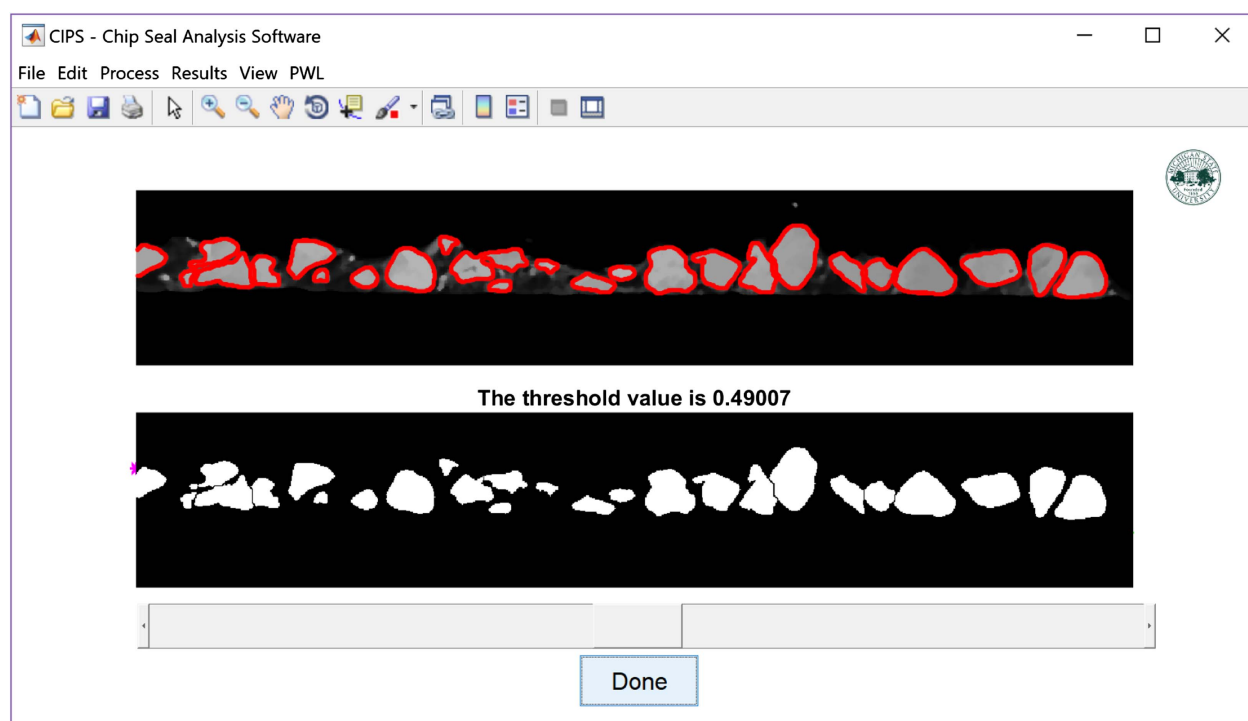


Fig. 9. Screenshot of CIPS software.

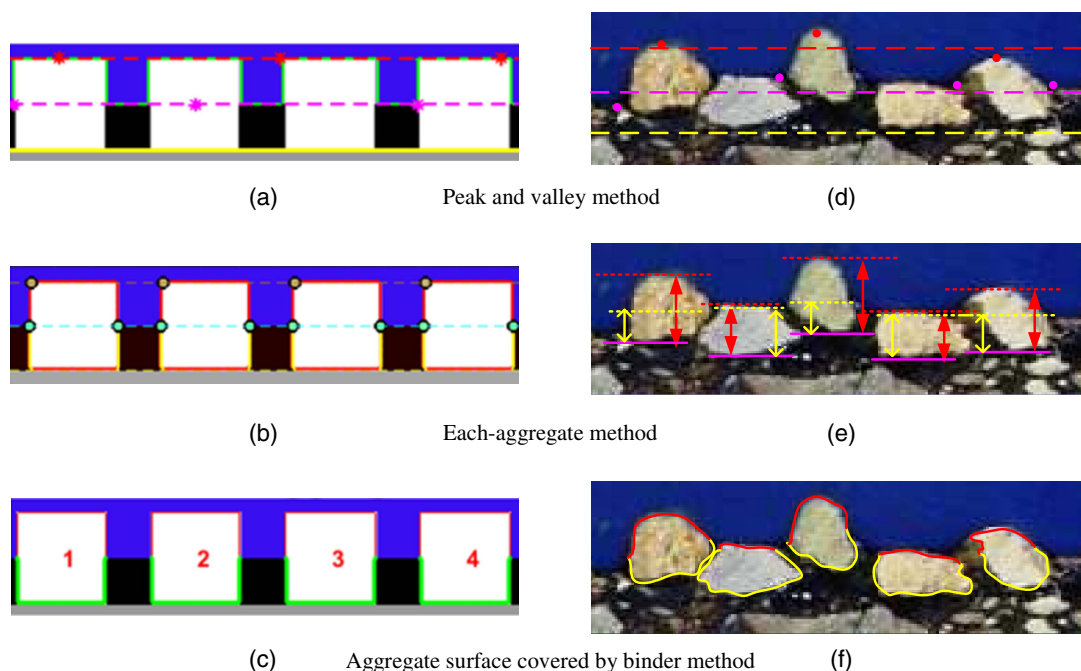


Fig. 10. Idealized as well as actual chip seal image validation: (a) $PE_{PV} = 49.99\%$ (CIPS) and $PE_{PV} = 50\%$ (actual); (b) $PE_{EA} = 50\%$ (CIPS) and $PE_{EA} = 50\%$ (actual); (c) $PC_{EA} = 49.88\%$ (CIPS) and $PC_{EA} = 50\%$ (actual); (d) $PE_{PV} = 51.04$ (CIPS) and $PE_{PV} = 51.98$ (manual), with error = 1.84%; (e) $PE_{EA} = 69.4$ (CIPS) and $PE_{EA} = 68.48$ (manual), with error = 1.33%; and (f) $PC_{EA} = 55.4$ (CIPS) and $PC_{EA} = 55.98$ (manual), with error = 1.08%.

the parameters PE_{pv} , PE_{EA} , and PC_{EA} were computed. Figs. 10(a–c) shows the results of the analyses, where an excellent match between the computed results and actual percent embedment of 50% has been obtained. Furthermore, a manual validation was also performed on actual chip seal images as illustrated in Figs. 10(d–f). For validation of PE_{pv} , first, the image was loaded to MATLAB software, then peak and valley points were manually selected on the image (using the function `getpts`), and their pixel (x - and y -) coordinates were obtained. Also, several points were selected on the substrate to obtain an average y -coordinate of the substrate. Then, from these coordinates, h_b (average binder height) and h_s (average aggregate height) were computed, and PE_{pv} was calculated using Eq. (1). In order to manually compute the PE_{EA} and PC_{EA} , the coordinates at perimeter of the aggregates as well as the perimeter coordinates that are covered by the binder were obtained by using a free-hand drawing function in MATLAB that provides the x - and y -coordinates of a line drawn on an image. From these coordinates, Eqs. (2)–(4) were used to calculate the PE_{EA} and PC_{EA} . As shown in Figs. 10(d–f), the parameters calculated by the CIPS software and manual calculations of the results match very well.

Traditional Methods for Estimating Percent Embedment

Sand Patch Test

The sand patch test is one of the most common methodologies used to compute road surface texture in the field [ASTM E965 (ASTM 2015b)]. However, in the case of chip seal applications, the sand patch test results are not enough to calculate the percent embedment of the aggregates. In fact, the mean texture depth obtained from the field test and average aggregate height must be used

together to calculate the percent embedment. The sand patch test can be summarized in the following steps:

1. Voids between aggregate particles are filled with the Ottawa sand that is spread on the surface of the chip seal application. Eq. (5) is used to calculate the mass of the Ottawa sand and its final value is the average of three replicates

$$M_O = M_{SO} - M_S \quad (5)$$

where M_O = mass of the Ottawa sand; M_{SO} = mass of the sample + Ottawa sand; and M_S = mass of the sample.

2. The volume of the Ottawa sand is then calculated because its density is known.
3. The following formula is used to calculate the mean texture depth (MTD):

$$MTD = \frac{4 \cdot V_{GS}}{\pi \cdot D^2} \quad (6)$$

where V_{GS} = volume of the Ottawa sand; and D = diameter of the sand patch that covers the chip seal surface.

Because aggregates typically tend to lie on their flattest side after compaction or exposure to traffic (McLeod et al. 1969), the average least dimension of the aggregates was estimated by using the following formula (Wood et al. 2006):

$$H = \frac{M}{1.139285 + 0.011506 \cdot FI} \quad (7)$$

where H = average least dimension (in.); M = median particle size (in.); and FI = flakiness index (%).

The percent embedment was calculated by using the following equation:

$$PE_{SP}(\%) = \frac{H - MTD}{MTD} \cdot 100 \quad (8)$$

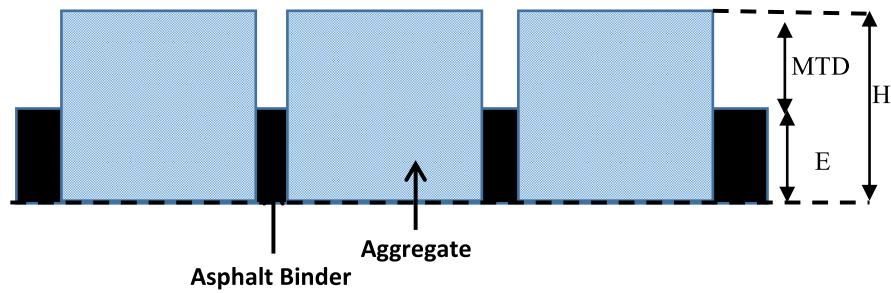


Fig. 11. Idealized chip seal cross section used in sand patch test.

Table 1. Average and standard deviation of the percent embeddings computed using various methods

Field section	Number of cores	Sand patch test (PE_{SP})		Laser texture scan (PE_{LT})		Percent embedment—peak/valley (PE_{PV})		Aggregate surface coverage (PC_{EA})		Percent embedment—each aggregate (PE_{EA})	
		Avg.	COV (%)	Avg.	COV (%)	Avg.	COV (%)	Avg.	COV (%)	Avg.	COV (%)
M-57	5	56.7	8.4	69.5	4.1	53.2	11.1	51.0	3.6	81.9	3.2
M-20	8	56.8	3.7	72.3	3.9	63.1	8.9	60.3	6.8	78.2	3.5
M-33	8	65.9	16.4	72.5	10.6	70.5	8.2	61.3	5.1	79.8	4.1
M-86	8	76.4	8.9	77.1	6.4	67.2	12.8	64.7	6.1	81.5	5.3
M-43	4	43.5	33.3	53.1	27.2	79.0	15.5	84.3	15.1	91.1	7.1
US-31	6	83.3	7.8	83.0	6.1	65.8	14.4	54.3	26.7	73.9	9.3
Total	39										

Note: Avg. = average; and COV = coefficient of variation (sample to sample variability).

where PE_{LT} = percent embedment from sand patch method; H = average least dimension (in.); and MTD = mean texture depth (in.) (Fig. 11).

Laser Texture Scanning

The laser texture scanner is another common method used in field for the estimation of the surface texture of chip seal applications. In the present study, an Ames model 9300 (Ames Engineering, Ames, Iowa) laser texture device has been used for this purpose.

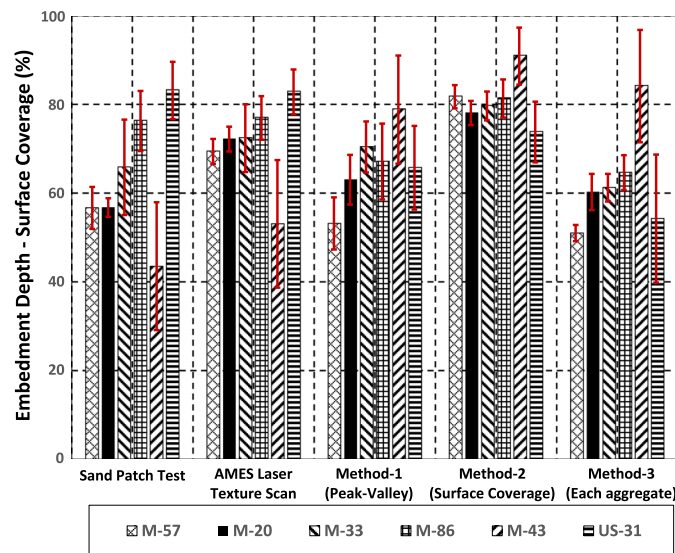


Fig. 12. Mean embedment depth for different methods from field samples.

This device is able to scan an area of 107.95 mm (length) by 72.01 mm (width). The laser texture meter divides the profile into 100-mm-long baselines to calculate the MPD. Then, two peak levels are determined for the first and second half of the baseline. The difference between peak levels and average height level is estimated and then averaged. This procedure is repeated for all baselines along the profile, and the average is taken as MPD or mean segment depth. After scanning, the equipment directly returns the MPD value.

It is well known that the MTD obtained from the sand patch test is not exactly equivalent to the MPD measured using the laser texture device. The ASTM E1845 (ASTM 2015a) specification

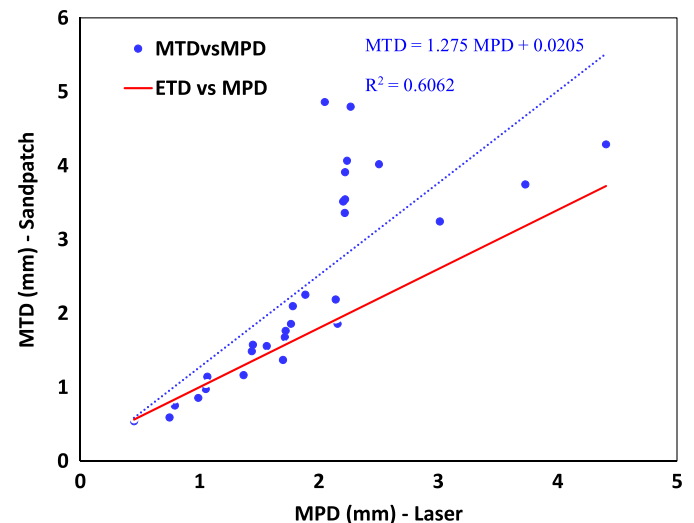


Fig. 13. Comparison of mean profile depth and mean texture depth measured on the chip seal sections utilized in this project.

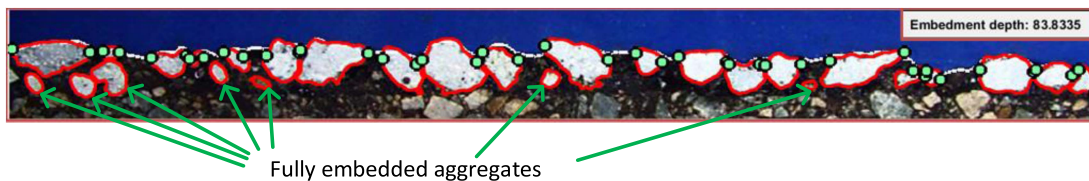


Fig. 14. Examples of fully embedded aggregates.

provides an empirical equation to estimate the texture depth (ETD) [Eq. (9)], which is a prediction of the MTD from MPD

$$\text{ETD} = 0.2 + 0.8 \cdot \text{MPD} \quad (9)$$

where ETD = estimated texture depth (mm); and MPD = mean texture depth (mm). Findings of the research performed by Freitas et al. (2008) showed that the MTD results obtained from the sand patch test are consistent with the ETD results estimated from MPD. Similar to the sand patch test formulation, the percent embedment is computed as follows:

$$\text{PE}_{\text{LT}}(\%) = \frac{H - \text{ETD}}{\text{ETD}} \cdot 100 \quad (10)$$

where PE_{LT} = percent embedment from laser texture meter; H = average least dimension; and ETD = estimated texture depth.

Analysis of Field Chip Seal Samples

Thirty-nine chip seal cores were collected from six different sections in Michigan (Table 1) and analyzed. The field sections were selected by the Michigan Department of Transportation (MDOT) crew. Before taking cores from the chip seal sections, the MDOT crew performed both sand patch tests and laser texture scans to measure texture depth of corresponding section. Then, chip seal samples were taken with a coring machine. Table 1 and Fig. 12 present the average and standard deviation of the percent embedment computed using various methods. Although the results from the sand patch test and laser texture scan are different, their trends are quite similar.

Furthermore, the laser texture scanning gives generally higher percent embedment compared with the sand patch test. The reason can be the inaccuracy of the empirical relationship between MPD and ETD, which is supposed to correspond to MTD obtained from sand patch test. Fig. 13 shows the comparison of mean profile depth and mean texture depth measured on the chip seal sections utilized in this project. As shown, the ETD equation ($\text{ETD} = 0.2 + 0.8\text{MPD}$) underestimates the MTD measured by the sand patch test when the texture depth is larger than 2 mm.

The results in Table 1 also indicate that the each-aggregate method (PE_{EA}) generally produces higher embedment depths compared with other methods. This is primarily because of the fully embedded aggregates (Fig. 14), which are better considered during calculations in this method. Additionally, the percent embedment from each aggregate (PE_{EA}) and aggregate surface coverage (PC_{EA}) methods seem to produce lower variability than the other methods. Also, these parameters are thought to be better than the rest of the parameters because they include analysis of each and every aggregate, rather than an overall average.

Conclusions

In this study, a novel procedure was developed to directly quantify embedment of aggregates in chip seals using image analysis techniques. The procedure includes obtaining 150-mm (6-in.) diameter field cores, cutting/slicing, taking digital images of the vertical faces, and computing the percent embedment using image analysis methods. In this research, three different image analysis algorithms, namely (1) peak valley method, (2) embedment of each-aggregate method, and (3) surface coverage area method, were developed. These algorithms were implemented into a standalone software package (herein called CIPS) and validated using idealized images with known percent embedment. Analysis of 39 field cores collected throughout Michigan revealed that the peak and valley method showed similar results as those obtained using the in situ sand patch test. This was expected because they both share same assumptions, such as the pavement surface being perfectly flat and ignoring the penetration of aggregates into the substrate. Analyses also revealed that the variability of the percent embedment obtained from the each-aggregate method was lower than the percent embedment obtained from the other methods. This method seems to be the most robust method in determining aggregate percent embedment.

Acknowledgments

The authors would like to thank the Michigan Department of Transportation (MDOT) for their financial support of this study.

References

- Abedini, M., A. Hassani, M. R. Kaymanesh, and A. A. Yousefi. 2017. "Low-temperature adhesion performance of polymer-modified bitumen emulsion in chip seals using different SBR latexes." *Pet. Sci. Technol.* 35 (1): 59–65. <https://doi.org/10.1080/10916466.2016.1238932>.
- Adams, J. M., and Y. R. Kim. 2014. "Mean profile depth analysis of field and laboratory traffic—Loaded chip seal surface treatments." *Int. J. Pavement Eng.* 15 (7): 645–656. <https://doi.org/10.1080/10298436.2013.851790>.
- Aktaş, B., M. Karaşahin, M. Saltan, C. Güler, and V. E. Uz. 2013. "Effect of aggregate surface properties on chip seal retention performance." *Constr. Build. Mater.* 44: 639–644. <https://doi.org/10.1016/j.conbuildmat.2013.03.060>.
- ASTM. 2015a. *Standard practice for calculating pavement macrotexture mean profile depth*. ASTM E1845. West Conshohocken, PA: ASTM.
- ASTM. 2015b. *Standard test method for measuring pavement macrotexture depth using a volumetric technique*. ASTM E965. West Conshohocken, PA: ASTM.
- Freitas, E. F., P. A. A. Pereira, M. L. Antunes, and P. Domingos. 2008. *Analysis of test methods for texture depth evaluation applied in Portugal*. Braga, Portugal: C-TAC—Comunicações a Conferências Nacionais, Universidade do Minho.
- Gaughan, R. 2001. *Austroroads provisional sprayed seal design method revision 2000*. Haymarket, NSW, Australia: Austroroads.

- Gransberg, D. D., and D. M. James. 2005. *Chip seal best practices*. Washington, DC: Transportation Research Board.
- Hanson, F. 1934. *Bituminous surface treatment of rural highways*. Wellington, New Zealand: Engineering New Zealand.
- Janisch, D. W., and F. S. Gaillard. 1998. *Minnesota seal coat handbook*. St. Paul, MN: Minnesota Dept. of Transportation.
- Kearby, J. 1953. "Tests and theories on penetration surfaces." In *Proc., 32nd Annual Meeting of the Highway Research Board*. Washington, DC: Transportation Research Board.
- Kim, Y. R., and J. Lee. 2006. *Quantifying the benefits of improved rolling of chip seals*. Raleigh, NC: North Carolina Dept. of Transportation, Research and Analysis Group.
- Kodippily, S., T. Henning, J. Ingham, and P. Cenek. 2010. "Modelling the flushing mechanism of thin flexible surface pavements." In *Proc., 2nd Int. Sprayed Sealing Conf.—Sustaining Sprayed Sealing Practice*. Port Melbourne, VIC, Australia: Australian Road Research Board.
- Lee, J., and R. Y. Kim. 2012. "Evaluation of polymer-modified chip seals at low temperatures." *Int. J. Pavement Eng.*, 15 (3), 1–10. <https://doi.org/10.1080/10298436.2012.655738>.
- McLeod, N., C. Chaffin, C. Holberg, V. Parker, J. Obrcian, W. Campen, and W. Kari. 1969. "A general method of design for seal coats and surface treatments." In *Proc., Association of Asphalt Paving Technologists Annual Meeting*. Lino Lakes, MN: Association of Asphalt Paving Technologists.
- Ozdemir, U. 2016. *An acceptance test for chip seal projects based on image analysis*. East Lansing, MI: Michigan State Univ.
- Roberts, C., and J. C. Nicholls. 2008. *Design guide for road surface dressing*. Berks, UK: TRL Limited.
- Shuler, S. 2011. *Manual for emulsion-based chip seals for pavement preservation*. NCHRP Rep. No. 680. Washington, DC: Transportation Research Board.
- Wielinski, J. C., J. Brandenburg, and J. Wissel. 2011. "The Monroe Michigan chip seal case study: An evaluation of multiple chip seals' cold weather field performance." In *Proc., Transportation Research Board 90th Annual Meeting*. Washington, DC: Transportation Research Board.
- Wood, T. J., D. W. Janisch, and F. S. Gaillard. 2006. *Minnesota seal coat handbook*. St. Paul, MN: Minnesota Department of Transportation.
- Zaniewski, J. P., and M. S. Mamlouk. 1996. *Pavement maintenance effectiveness—Preventive maintenance treatments*. Washington, DC: Federal Highway Administration.